

AERODYNAMIC ANALYSIS OF THE FLOW CHARACTERISTICS OF A DELTA-CANARD
CONFIGURATION

A. Ferretti and A. Salvatore

AERITALIA DEFENCE AIRCRAFT GROUP

Torino, Italy

ABSTRACT

A complete cycle of aerodynamic analysis of the local flow characteristics on a delta-canard aircraft configuration has been performed through the examination of wind tunnel and flight data covering subsonic-transonic and supersonic regimes. A pressure plotting wind tunnel model scale 1:13, designed and manufactured by AERITALIA, has been tested in different entries in the ARA/RAE (U.K.) wind tunnels.

Flow characteristics have been investigated in the whole Mach-alpha range of interest, analyzing development of vortex flow on the wing surface and the effects of canard on it.

Key aerocharacteristics, like trailing edge pressure and minimum pressure coefficient on the wing, have been identified and correlated to the insurgence of peculiar flow structures obtaining a prediction criterion of transition from attached to vortex flow.

The availability of in-flight pressure measurements over the flying surfaces of BAe E.A.P. demonstrator aircraft has allowed a comparison of wind tunnel versus flight data, evaluating the effects of varying the Reynolds number.

A comparison of the experimental results with computational estimates has been carried out in order to assess the reliability of the theoretical methods in predicting complex 3D flow fields.

1. INTRODUCTION

The design of defense aircraft having to fulfill requirements in supersonic regime, as cruise or acceleration, leads to consider high swept wing configurations with low aspect ratio.

Such wing planforms present the potential of achieving high aerodynamic efficiency minimizing drag due to lift through an appropriate twist and camber distribution ensuring attached flow and favourable trim drag in supersonic flight condition.

However multiple design points have to be considered for a defence aircraft; emphasis is placed on transonic manoeuvre characterized by high lift coefficient (CL) operation where different camber and twist distributions are required.

As a result, wings suitable for efficient supersonic cruise develop leading edge (l.e.) separation and vortex flow at relatively low angle of attack in subsonic-transonic flight conditions.

Potential degradation of drag polars that generally reflect very little l.e. suction

recovery is experienced in this case.

However, advantages can be achieved by a careful design incorporating means for "controlling" the vortex flow; devices such as forebody strakes, canards, vortex flaps and their integration with variable camber devices on the wing surface can provide improvement in the high lift, stability and control, and buffet characteristics of the aircraft.

Great importance is therefore attributed in the prediction of transition from "attached" flow to vortex flow on aircraft featuring high swept wings: in fact even though "controlled" vortex can improve manoeuvrability highly integrated design is required to avoid other aerodynamic shortcomings.

This paper presents the results of an investigation carried out in Aeritalia, Defence Aircraft Group, on the wing flow characteristics of a defence aircraft featuring a double delta-canard configuration.

Investigation has been carried out aiming at a better understanding of the causes leading to vortex flow development on the wing at transonic flight conditions; nevertheless subsonic and supersonic conditions have been analyzed as well.

A deep analysis correlating overall aerocharacteristics (lift and moment coefficients CL vs α , CM vs α) with the wing flow field structure and fluidodynamic characteristics has been attempted to the aim of detecting "key" aero-parameters helpful in the prediction of l.e. separation and vortex flow development.

The results presented are based on work that began in late 1985 in Italy in support to the B.A.e (U.K.)- AIT (IT) E.A.P. programme.

In this context pressure data were generated by AIT by means of a pressure plotting wind tunnel model since 1986, and later on by B.A.e that flew a demonstrator aircraft with a sophisticated pressure acquisition system. Data relevant to other high swept wings have been utilized as well.

In the paragraph 4.1.2. a preliminary criterion for the prediction of transition from attached to vortex flow in subsonic-transonic condition is presented; the availability of pressure data on other wing planforms could consolidate its validity.

Furthermore the applicability of theoretical methods combined with the prediction criterion is presented highlighting the capability to predict vortex flow occurrence at an early stage in the design process.

2. MODEL TESTED

The data presented in this paper are relevant to wind tunnel experimental investigation on E.A.P. Model 9, designed and manufactured in AIT GAD. The model reproduces a double-delta canard configuration (fig.1) with two coupled bidimensional air intakes in ventral position.

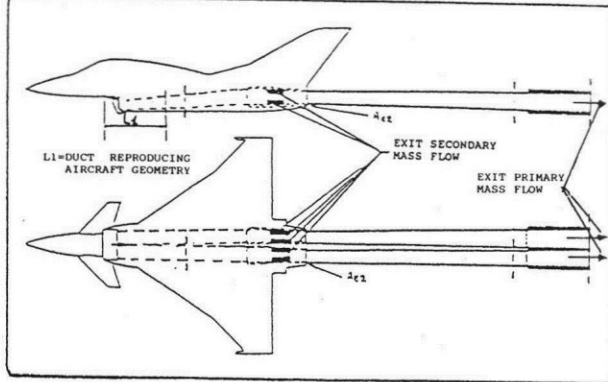


FIG.1
MODEL SCHEME

It has been designed for the pressure distributions measurements by the realization of 650 pressure points distributed all over the surface (tab.1).

Wing upper surface, port side	126 points
Wing lower surface, starboard side	110 points
Fuselage, port side	200 points
Foreplane upper surface, port side	31 points
Foreplane lower surface, starboard side	28 points
Fin and rudder, port side	69 points
Airbrake, upper and lower surfaces, port side	12 points
Küchemann tip, upper and lower surfaces, starboard side	4 points
Mass flow instrumentation, 4 stations	24 points

TAB.1
PRESSURE TAPS DISTRIBUTION

The pressure points location on the wing upper surface, port side, is reproduced in fig.2 in which ten instrumented chordwise sections (STU2+STU11) are visible.

The model includes a five component balance, located in the forward part of the double sting in order to validate loads calculated by pressure integrations, both in subsonic-transonic and supersonic regimes.

Although the small scale, 1:13, the model has been conceived to contain all the instrumentation needed for pressure measurements in addition to a special duct to simulate different mass-flow conditions. Four stations instrumented with 24 pitot/static pressure points allow the measurement of mass-flow, deemed an important parameter influencing overall aerocharacteristics in highly integrated intake configurations (fig.3).

Model 9 has been tested, in different entries, in subsonic-transonic and in supersonic wind tunnels (w.t.), resp. ARA and RAE in Bedford (UK), since 1986 to 1989 (fig.4a).

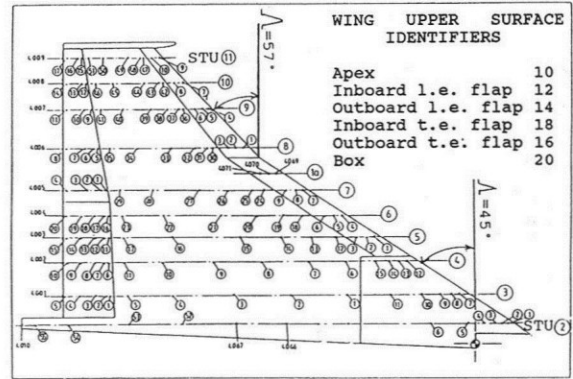


FIG.2 UPPER SURFACE PORT WING PRESSURE POINT LOCATIONS

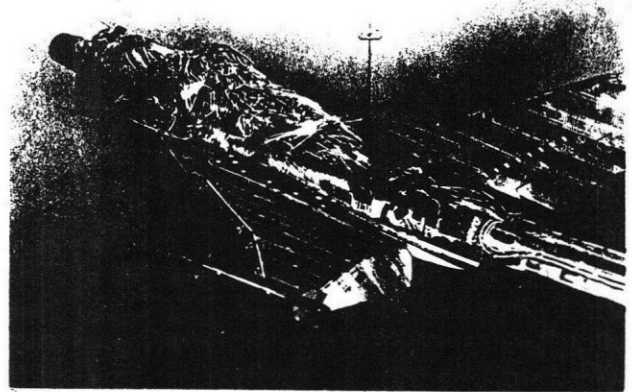


FIG.3
E.A.P. M9 INSTRUMENTATION

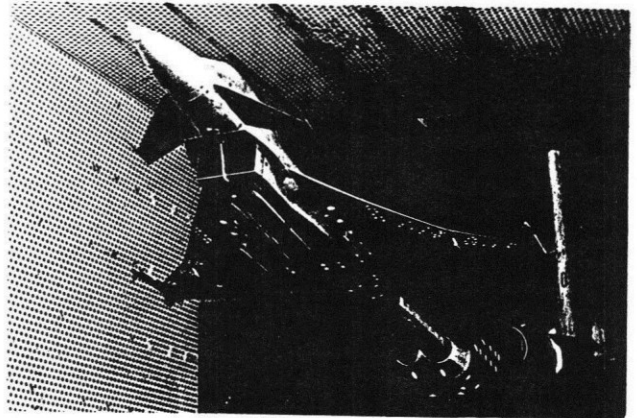


FIG.4 a
E.A.P. M9 IN TRANSONIC WIND TUNNEL

Comparison has been also carried out between w.t. and flight pressure data measured by piezoelectric sensors on the E.A.P. demonstrator aircraft (fig.4b), in context of an AIT-GAD and BAE aerodynamic collaboration programme.

The comparison between w.t. and flight data has allowed to assess the reliability of defining loads by integrating pressure obtained on a scaled model highlighting areas where extrapolation to full scale aircraft needs monitoring due to the Reynolds number ($Re_{n'}$) effects.

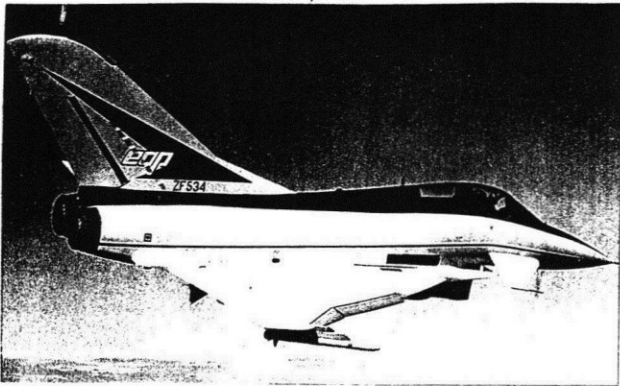


FIG. 4b
E.A.P. DEMONSTRATOR AIRCRAFT

3. E.A.P. WIND TUNNEL/FLIGHT DATA COMPARISON

E.A.P. Flight Loads Survey consisted of a series of flights dedicated to aerodynamics loads evaluation by means of wing, foreplane, fuselage and fin pressure measurements and integration. Comparison with analogous w.t. data obtained by testing of E.A.P. Model 9 has evidenced a satisfactory trend in pressure distributions all over the wing chordwise stations.

M=0.8, 20KFT, WUT, L.E.=0 ALFA 2.91

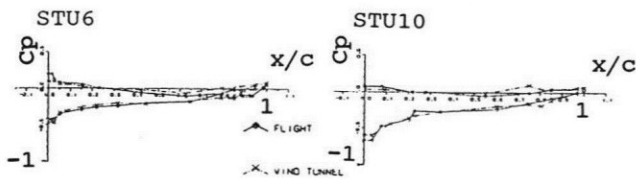


FIG. 5
COMPARISON WIND TUNNEL AND FLIGHT DATA

M=1.20, 30KFT, WIND UP TURN, L.E.=0 ALFA 6.02

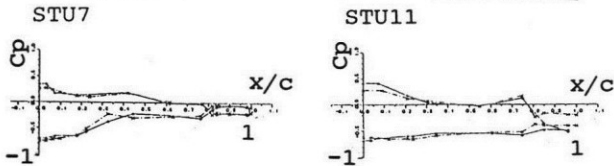


FIG. 6a

Mach=1.35 Beta = .10 $F_p = -1.44$ $F_{lap} = -6.23$ ALPHA=4.61
▲ flight data
□ ARA/RAE w.t.

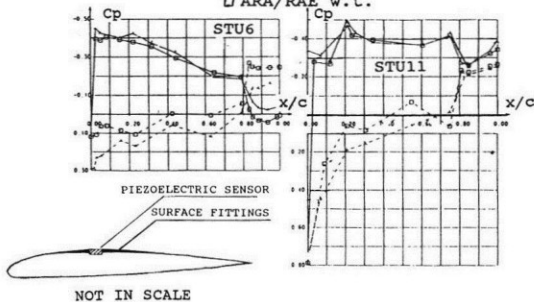


FIG. 6b
COMPARISON WIND TUNNEL AND FLIGHT DATA

Figures 5 and 6 present w.t. and flight wing pressure distributions for different Mach numbers (M) proving the reliability of the acquisition system set-up for in flight measurements. In this case a disc fairing (fig.6b downleft), whose size were chosen on the basis of theoretical - experimental investigations, allowed to minimize the disturbances induced by the piezoelectric sensors placed on the aircraft surfaces.

3.1. REYNOLDS NUMBER EFFECTS

In order to evaluate the effects of air viscosity about pressure coefficients, w.t. tests have been carried out fixing the transition on the wing and varying Re_n : $6.1E6$, $11.9E6$, $15.4E6$, and at $6.1E6$ transition free.

A comparison between the results in this way obtained and flight ones has allowed to justify some discrepancies in suction peaks of pressure distribution near l.e.. The analysis has been carried out at $M=0.80$ evaluating integral (CL,CM) and pressure coefficients (Cp) along the chord at fixed stations and angle of attack. Since the flow is attached, there is no dependence of Cp vs Re over all spanwise stations near l.e. (for the evaluation of M, α conditions from attached to vortex flow see par. 4.1.). When the transition to vortex flow is completed there is a remarkable increasing of |Cp| value with Re_n increasing (fig.7).

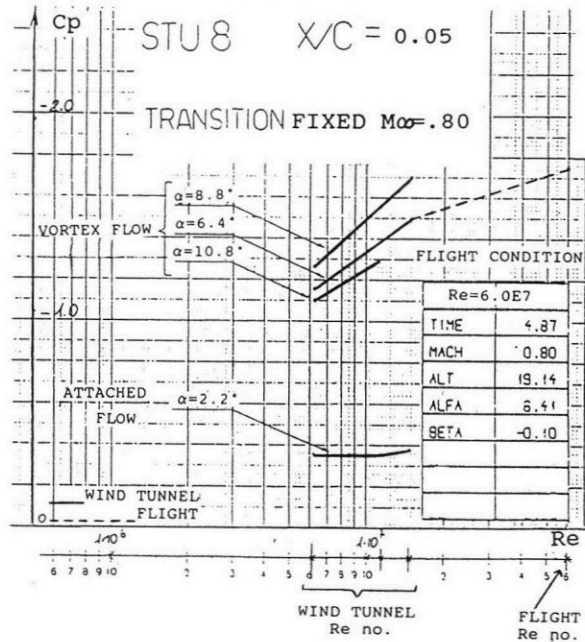


FIG. 7

Re no. EFFECTS ON PRESSURE COEFFICIENT

Flight tests have confirmed this trend; in fact flight pressure distributions gathered at $Re=60E6$ have shown a more intensive suction peaks than w.t. distributions, M, α conditions being equal (fig.8). Increasing x/c towards trailing edge (t.e.), the dependence of Cp with respect to Re_n becomes very weak as presented in fig.9.

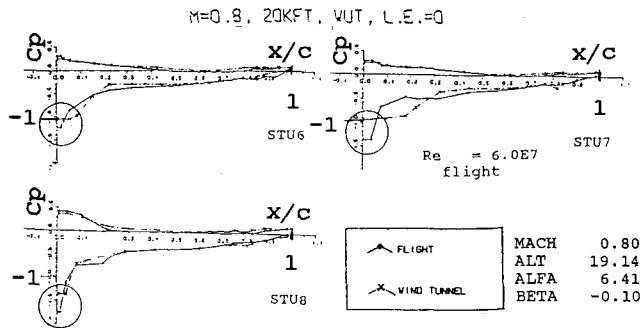


FIG. 8
Re no. EFFECTS ON L.E. SUCTION

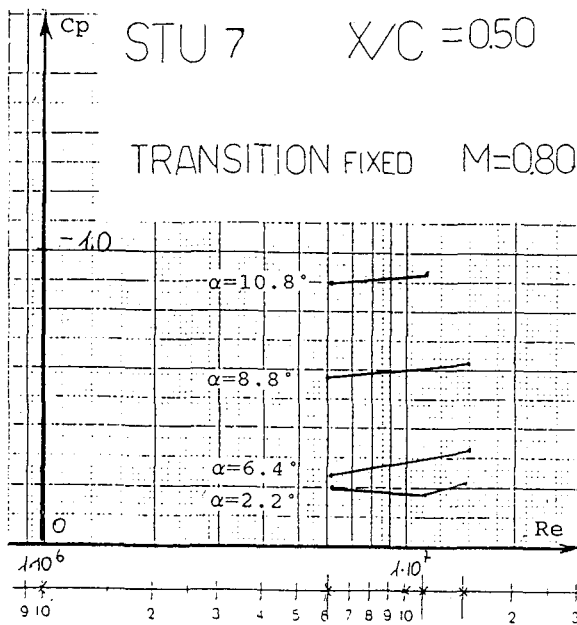


FIG. 9
Re EFFECTS ON PRESSURE COEFFICIENT

The comparison with flight data at these x/c confirms the no dependence above mentioned (see also fig.8).

The transition strips simulate a pseudo Re n° higher than the transition free case in the l.e. area. In fig.10a C_p vs y at two fixed X stations is represented; in the inboard wing portion the flow is attached (fig.10b) and the dependence of C_p respect to Re n° is negligible, while, in the outboard wing portion, that is characterized by vortex flow with l.e. separation, there is an increasing of C_p value, confirming the trend of increasing C_p with increasing Re n° seen before.

Although C_p value is strongly dependent on Re n° when the flow is detached at l.e., the longitudinal coefficients C_L and C_M evidence a slight dependence, consistent, in any case, with the previous results. The conditions of transition from attached to vortex flow have been often mentioned; in the next chapter it will be explained how to evaluate these conditions by the analysis of pressure distributions.

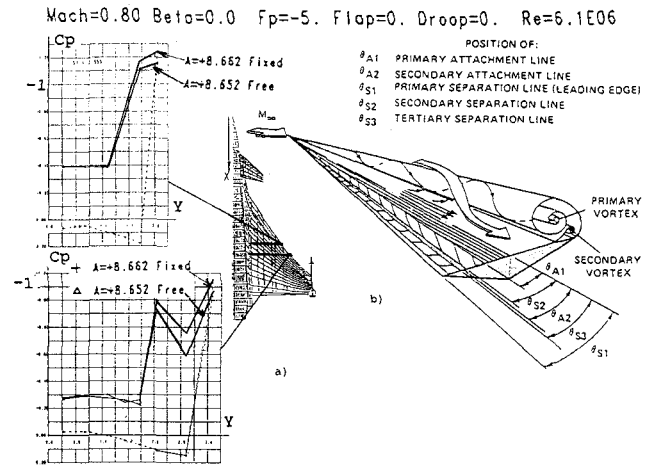


FIG. 10
Re EFFECTS ON PRESSURE COEFFICIENT

4. TRANSITION FROM ATTACHED TO DETACHED FLOW AT LEADING EDGE

4.1. SUBSONIC-TRANSONIC REGIME

Delta wing configurations are characterized by attached flow at l.e. only for moderate α, M , becoming vortical with increasing of these conditions.

By the analysis of pressure distributions of E.A.P. M 9 it has been possible to find the conditions leading to vortex flow development. In fig.11a the evolution of C_p vs x/c for attached flow is presented. A sudden change in pressure distribution shows up with vortex flow onset: a strong l.e. suction and a following intensive recompression gradient take place (fig.11b).

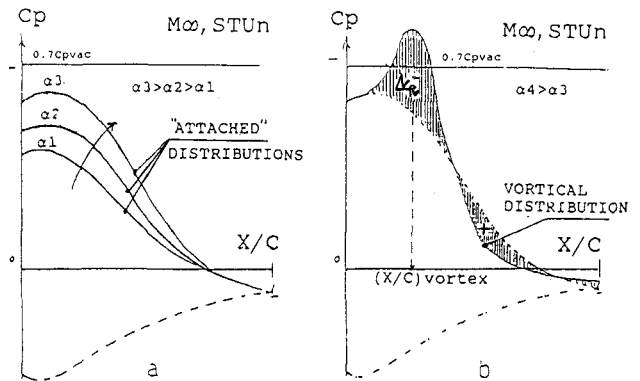


FIG. 11
FROM ATTACHED TO VORTICAL FLOW DISTRIBUTION

At fixed M , the transition starts at wing tips and, increasing α , propagates inboard. In fig. 12 is presented the vortex-core projection over the wing (locus of C_{pmin}) at an angle of attack for which vortex flow is dominant all over the wing.

There are two vortical structures more inclined with respect to l.e sweep angle confirming the classical evolution of the vortex sheet and the decreasing of vortex strenght (C_{pmin}) moving away from the wing apex (vortex1), and from the crank (vortex2).

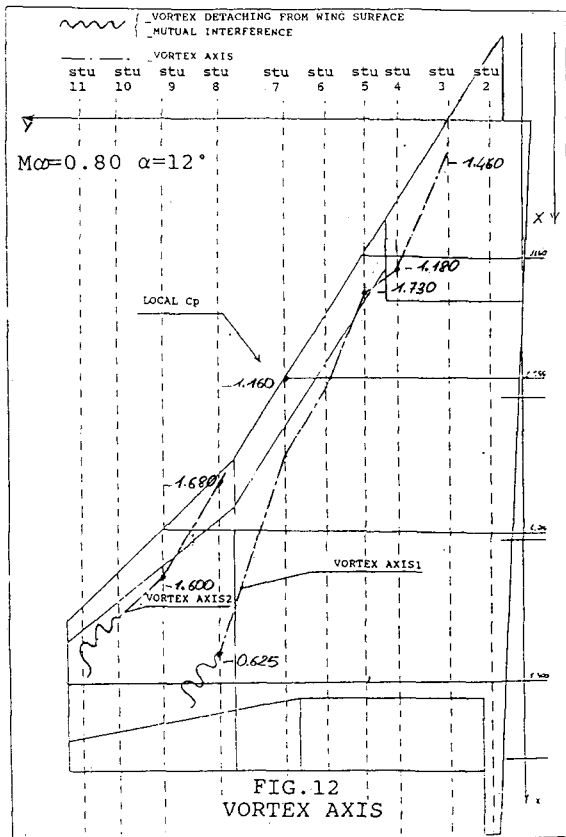


FIG. 12
VORTEX AXIS

4.1.1. TRAILING EDGE PRESSURE DIVERGENCE

A recurrent relation between a negative pressure shift at t.e. and the growing of vortex flow has been found analyzing sectional pressure distributions (fig.13).

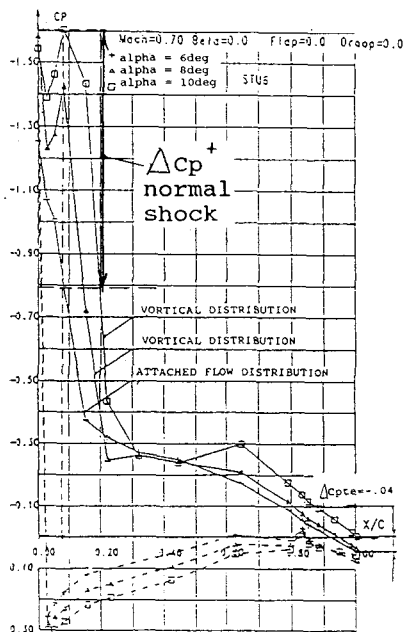


FIG. 13

PRESSURE DISTRIBUTIONS

In particular, when C_{pte} shift in the order of $\Delta C_{pte} = -.04$ is experienced, the transition from attached to vortex flow is completed. For traditional wing

configurations, $\Delta C_{pte} = -.04$ is related to the worsening of shock induced separation, and consequently, to the insurgence of buffet.

Starting from this consideration the analysis has been aimed to look for the same kind of correlation; but, surprisingly, for delta configuration or for configurations characterized by vortex flow, $\Delta C_{pte} = -.04$ is not related to a shock strenghtness being, on the contrary, linked to the transition from attached to vortex flow (detached at l.e.). In fact the pressure recovery after C_{pmin} is largely greater than maximum recompression gradient achievable through a normal shock (fig.13).

This is very important because once "criticity" is spread out over a certain wing portion, the angles of attack (α_{cr}) for which $\Delta C_{pte} = -.04$ are well correlably with the angle of attack (α_{kink}) of loss of linearity in the integral coefficients C_L and C_M ; this is true for traditional and delta wing configurations.

In fact plotting, for E.A.P. M 9, α_{cr} vs spanwise stations and placing on α_{kink} , it is visible, increasing α , a clear relation between the expansion of divergence from tip to root and kink incidences.

These kinks become more and more intensive increasing α (fig.14).

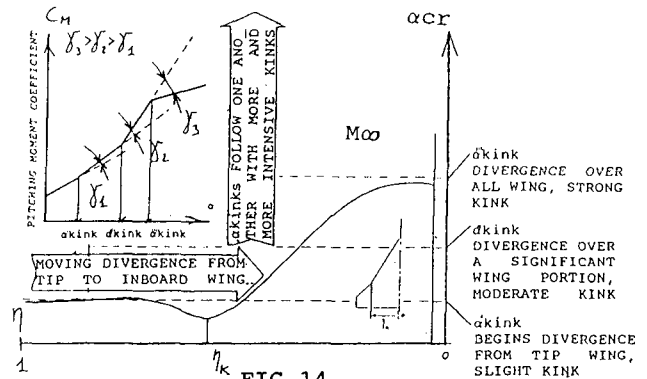


FIG. 14

COMPARISON α LOSS OF LINEARITY (α_{kink}) AND α DIVERGENCE AT T.E. (α_{cr})

Summarizing, for delta configurations, divergence at t.e. is a signal of incipient transition of flow typology; the setting up of vortex flow causes a loss of linearity in longitudinal coefficients that becomes important when a significant wing portion is interested by divergence phenomenon.

In condition of strong interaction between potential and viscous flow, the aircraft is stressed by an aerodynamic force against which it reacts with aeroelastic vibrations.

This phenomenon, called buffet, limits the aircraft manoeuvrability and its performance. Relating buffet-onset to loss of linearity, i.e. with birth of vortex flow, it is possible, predicting attached to vortex flow transition, to build a prediction criterion for buffet-onset.

4.1.2. CRITERION FOR PREDICTING TRANSITION FROM ATTACHED TO VORTEX FLOW

The onset of vortex flow is identified by a strong peak of negative pressure near l.e. in the section examined. This peak (identified by C_{pmin}) grows, increasing α , with decreasing slope till a minimum value ($(C_{pmin})_{max}$); for higher α , smaller suction peaks are evidenced (fig.15).

Mach=0.80 Beta=0.0 Flap=0.0
 + ALPHA = 10
 Δ ALPHA = 12
 □ ALPHA = 14
 ∟ ALPHA = 16

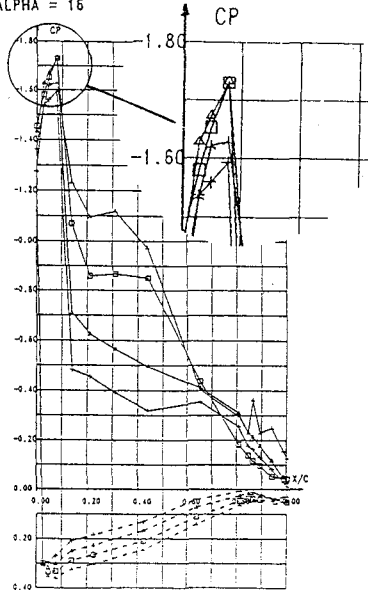


FIG. 15
Cpmin TREND

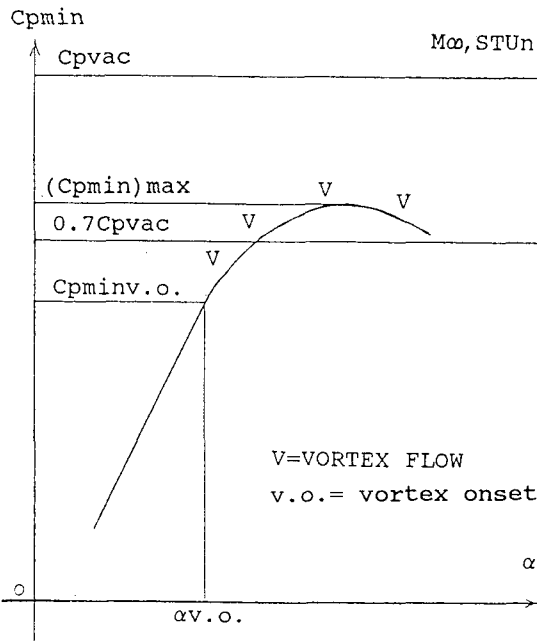


FIG. 16
Cpmin VERSUS α

Referring to plots such as presented in fig.16, it has been calculated, for all

the instrumented sections and for M ranging from 0.60 to 0.95, the following ratio:

$$f(y) = \frac{C_{pminv.o.}}{C_{pvac}} \quad (1)$$

where $C_{pminv.o.}$ is the pressure coefficient corresponding to vortex-onset and C_{pvac} is corresponding at vacuum (this last value depends only to M). C_{pvac} has been chosen like reference pressure term because this value can never be overtaken. It's worthwhile now to remark that, for traditional wing configurations, the experience tell us that minimum Cp value obtainable is never lower than $0.7C_{pvac}$, while in delta configurations, such as E.A.P. M 9, this level is often overtaken, particularly at higher M (fig.17).

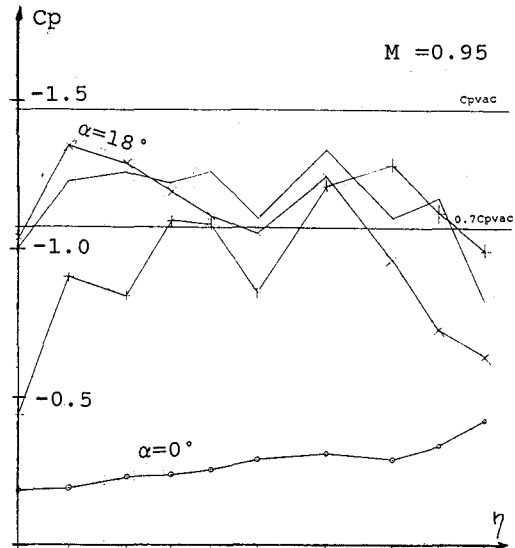


FIG. 17
NEGATIVE MINIMUM PRESSURE PEAKS

At fixed M, the value obtained by (1) is almost constant in all the spanwise sections; plotting now a mean value ($f(M)$) of this ratio versus M, it is possible to build a curve that contains in itself an important concept (fig.18).

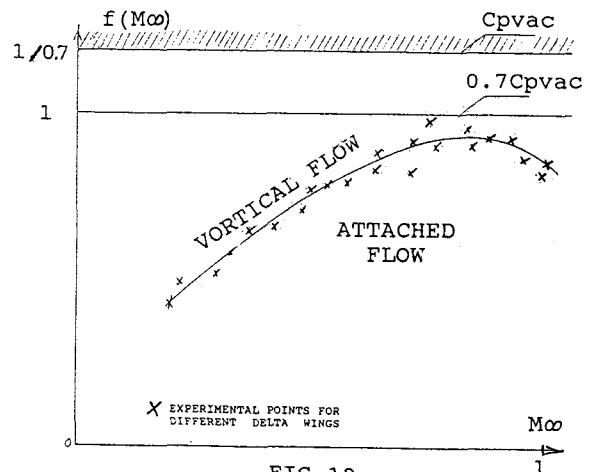


FIG. 18
FUNCTION OF FLOW TRANSITION

The $f(M)$ function divides the plane in two

parts in which two types of flow exist. Below it the flow is attached, while above, near the border, vortex flow is dominant.

The key rule in $f(M)$ function is its not dependence on wing geometrical characteristics such as l.e. radius, l.e. sweep angle, airfoil thickness ect, ect... Geometry takes part only in defining the conditions α, M at which the transition from attached to vortex flow occurs ($C_{pmin.v.o.}$); it doesn't influence, at fixed M , the value of $C_{pmin.v.o.}$ itself, the ratio (1) being a pure fluidodynamic relation well-founded for delta wing configurations.

The numerical form of this function becomes more and more accurate if we consider a great number of delta wings (greater number of points on $f(M)$ - M plane produces a more defined interpolation function).

Data obtained by the analysis of two different models characterized by vortex flow, E.A.P. M 9 and M 165 (ARA model relating to European Research I.E.P.G. TA 15, fig.19) have given the same results confirming the overall consistency of the criterion.

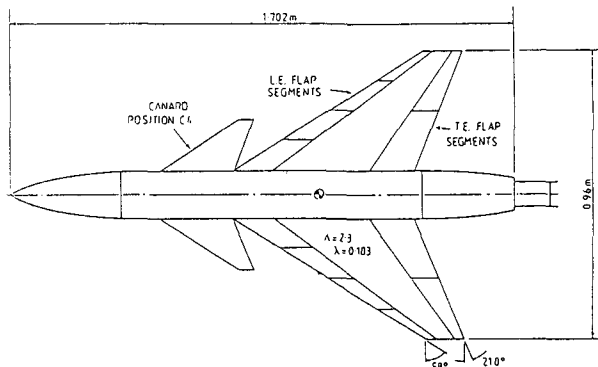


FIG. 19

M165 GENERAL LAYOUT OF MODEL.

The implication on the aerodynamic design process is evident: theoretical estimates of potential pressure distributions, linked to the correlation criterion, allow to predict the vortex flow onset on delta wing configuration or for a wing featuring vortical flow.

A comparison of the experimentally derived results with computational estimates has been carried out in chapter 6 in order to asses the reliability of the theoretical methods in predicting complex 3D flows.

4.2. SUPERSONIC FLOW

4.2.1. SUPERSONIC FLOW FIELD STRUCTURE

In order to provide a systematic analysis of the flow field structure in supersonic flow, a comparison of the experimental data with the Stanbrook and Squire α_n vs M_n diagram for rounded l.e. wings has been attempted. This methodology is applicable, a priori, only to delta wing configuration but the extrapolation of some qualitative results on E.A.P. double delta wing configuration seems to be reasonable particularly for the higher

sweep angle wing portion.

The normal Mach number M_n and normal angle of attack α_n are defined as:

$$M_n = M [1 - \sin^2 \Lambda \cos^2(\alpha + \beta)]^{1/2} \quad (2)$$

$$\alpha_n = \arctg[\tg(\alpha + \beta) / \cos \Lambda] - \arctg[\tg \beta / \cos \Lambda] \quad (3)$$

where Λ is the l.e. sweep angle and β is the upper surface wedge angle in the plane of symmetry (fig.20), here assumed to be zero.

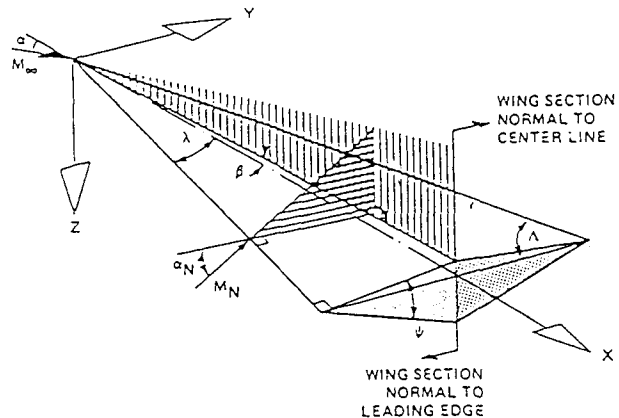


FIG. 20

DELTA WING GEOMETRY AND FLOW COMPONENTS

The parameter M_n describes the position of the sonic line, i.e. whether the l.e. is inside or outside the Mach cone. Using this criterion together with the normal angle of attack, flow field features can be recognized as a first approximation (fig.21), the diagram being divided into regions of attached and separated flow at the l.e..

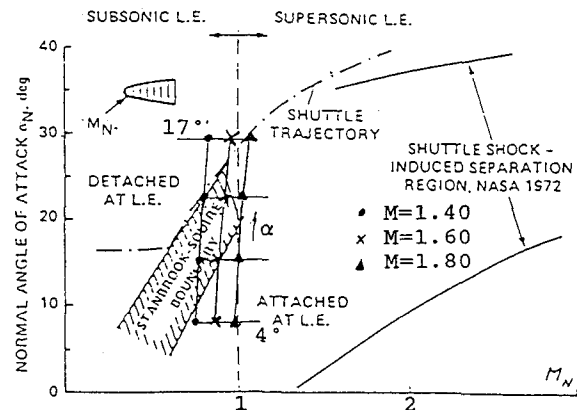


FIG. 21 BOUNDARY BETWEEN DETACHED AND ATTACHED LEADING-EDGE FLOW FOR ROUNDED EDGES

The Stanbrook and Squire boundary defines a region where both separated and attached flow may be found, its broadness resulting from evaluating different Re_n cases and different l.e. radii. With respect to a sharp edge wing, a rounded edge one tends to delay l.e. separation to higher angle of attack.

The experimental supersonic data, placed

on an-Mn diagram (fig.21), identify the flow structure, perfectly according to the information derivable from pressure distributions. It is confirmed, in fact, a defined vortex structure for lower supersonic M, high α (l.e. separation, detached at l.e.) that disappears increasing M (attached at l.e. with local Prandtl-Mayer expansion, fig.22).

Beta=0.0 Fp=-5. Flap=0. Droop=0.
 + A=17.606 M=1.40 EAP M9 RAE SWT
 Δ A=17.265 M=1.60
 □ A=17.023 M=1.80

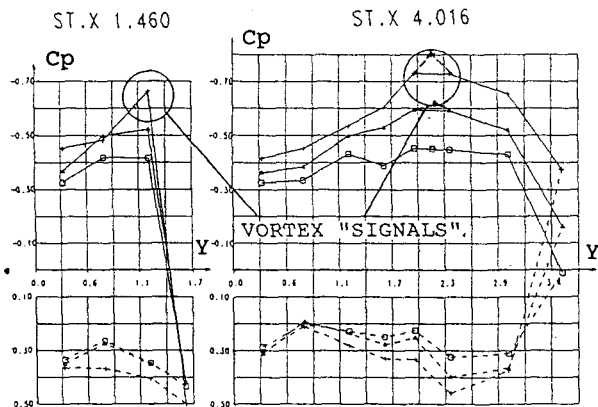


FIG.22
 SUPERSONIC PRESSURE DISTRIBUTIONS

Moreover the spanwise pressure distributions on both the upper and lower surface show, as expected, scaled pressure coefficients with increasing M all over the range of angles of attack. Referring the longitudinal coefficient CN, the normal force vs incidence shows a decreasing slope with increasing M, as expected (fig.23).

Beta=0.0 Foreplane=-5. Flap(1/B,0/B)=0.0
 + Mach=0.80 Δ Mach=1.40 Droop(1/B,0/B)=0.0
 □ Mach=1.60

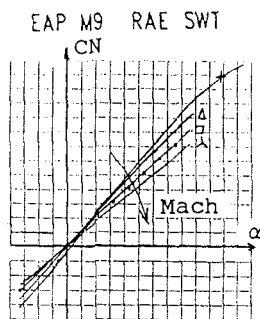


FIG.23
 LONGITUDINAL COEFFICIENT "CN"

5. FOREPLANE EFFECTS

In order to provide an outline of the foreplane (f/p) induced effects on the wing, an analysis of its influence on the pressure distributions in subsonic and transonic regimes has been carried out giving particular emphasis to the t.e. divergence seen in previous paragraphs.

5.1. SUBSONIC-TRANSONIC FLOW REGIME

When the foreplane trailing vortex interacts with wing flow field, it causes a change in pressure distributions, particularly in the spanwise stations range interested (for E.A.P. M 9: STU3, STU4, STU5, fig. 24).

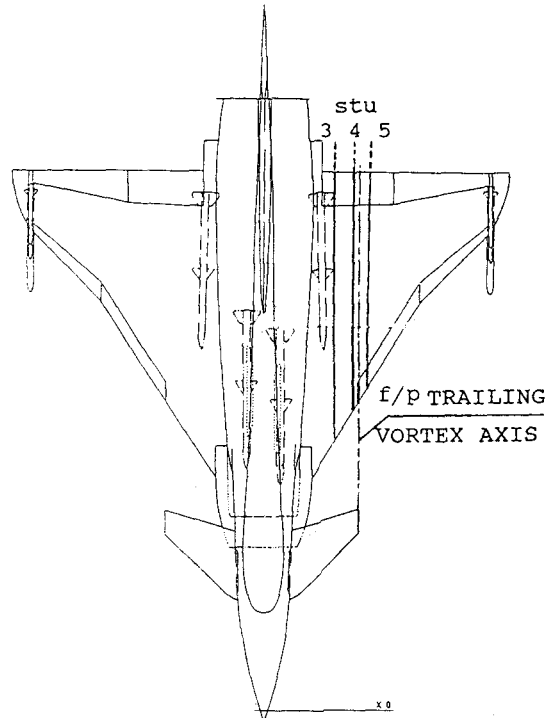


FIG.24
 FOREPLANE INFLUENCE ON THE WING

Because of the short-coupled configuration, the interaction between trailing vortex and l.e. vortical flow is significant and it causes a change of the pressure peaks associated with the vortex in the influenced sections. In particular, due to the trailing vortex induced velocity, there is an increasing of $|C_{pmin}|$ on STU 3, and a linear decreasing of it from STU4 to STU5 (see decreasing trend of C_{pmin} value on vortex axis in fig.12).

Moreover the x/c of C_{pmin} (vortex peak) on STU4 is shifted towards t.e. because of the interaction of the two vortex; a qualitative interpretation of this shift is illustrated in fig. 25.

It is worthwhile to be mentioned that f/p trailing vortex reaches the t.e. of the wing only in limited incidence ranges.

In these cases, plotting t.e. pressure coefficient versus span and versus incidence, it is possible to identify angle of attack range ($\Delta\alpha$) and span range (Δy) of influence of f/p trailing vortex on the whole wing (fig. 26).

This evaluation is important in order to correctly evaluate the incidences of divergence at t.e., α_{cr} (see par.4.1.1.).

In fact, $\Delta C_{pte} = -.04$ is a negative shift to associate to a global change of pressure distributions due to the transition from attached to vortical flow and not attributable to the local effects due to a sliding trailing vortex.

Therefore, about evaluation of α_{cr} in the presence of f/p, it is necessary to extrapolate, in $\Delta\alpha_v$, the curve C_{pte} vs α , such as in fig.26c (dash line), avoiding

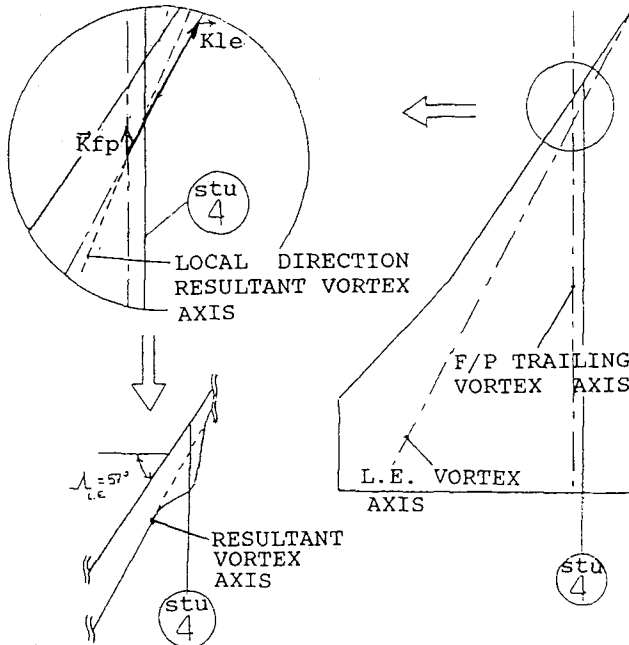


FIG.25

INTERACTION BETWEEN TRAILING AND L.E. VORTEX

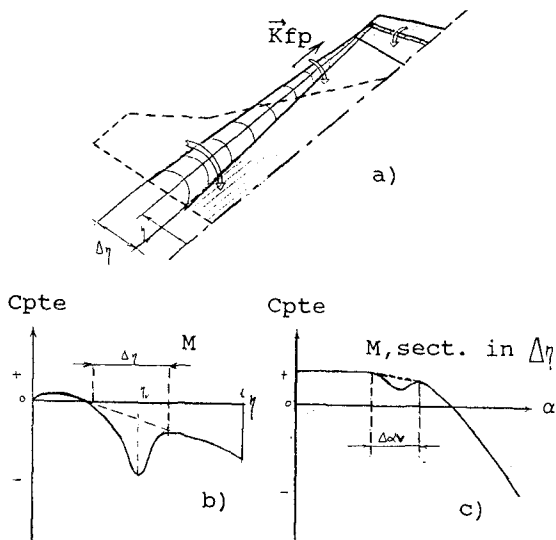


FIG.26

RANGES OF INFLUENCE OF F/P TRAILING VORTEX

underestimate of α_{cr} .

At fixed α, M conditions, the position at which the f/p trailing vortex leaves the wing surface (X_d , fig.27) is dependent on f/p setting δ_f .

F/p, with its setting, produces a "control system" of pressure distributions because it defines the amount of $\Delta C_{p_{f/p}}$ (pressure contribution of f/p trailing vortex alone) and the value of X_d (fig.27).

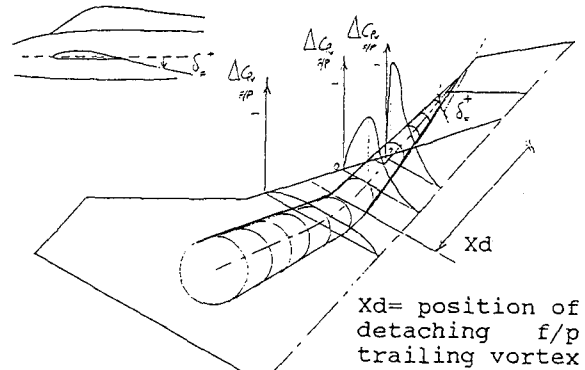


FIG.27
F/P TRAILING VORTEX

6. THEORETICAL ESTIMATES OF FLOW FIELD

An assessment on the capability to predict transition from attached to vortex flow by utilizing the criterion dealt with in par.4.1.2. needs a verification of the computational method reliability.

It is well known that efficient and robust CFD methods have been recently developed allowing resolution of Euler equations on complex 3D configurations featured by vortical flow; on the contrary, the background, the prediction criterion is based upon, suggests the possibility to utilize "relatively simple and cheap" potential codes exclusively to predict attached flows until α, M conditions of vortex onset defined by the prediction criterion itself.

In this view, a comparison of the experimentally derived results with computational estimates obtained with a potential code (panel method "NLRAERO") has been carried out.

At first, a matching of theoretical and experimental results on a basic configuration has been performed to assess the suitable mathematical model definition (fig.28).

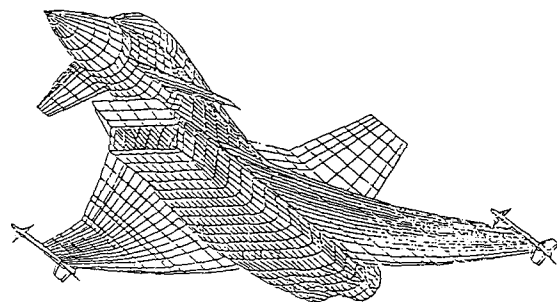


FIG.28

MATHEMATICAL MODEL

Subsequently, a comparison of pressure distributions has been analyzed. The experimental results at $M=0.60$ are compared in fig.29 with theoretical estimates, evidencing a good accordance.

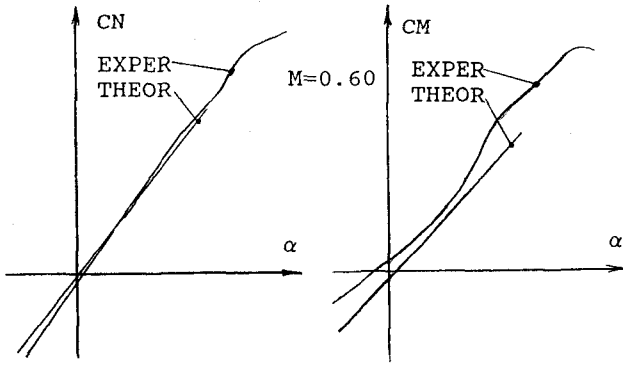


FIG. 29

COMPARISON THEORETICAL TO EXPERIMENTAL RESULTS

Matching process, carried out at $M=0.60$, proved to be acceptable looking at the comparison performed at higher Mach numbers as presented in fig.30.

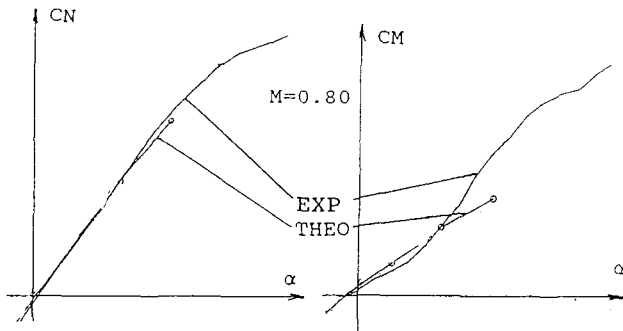


FIG. 30

COMPARISON THEORETICAL TO EXPERIMENTAL RESULTS

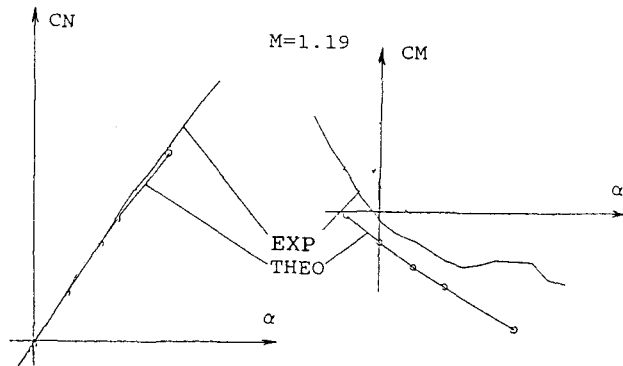


FIG. 30

COMPARISON THEORETICAL TO EXPERIMENTAL RESULTS

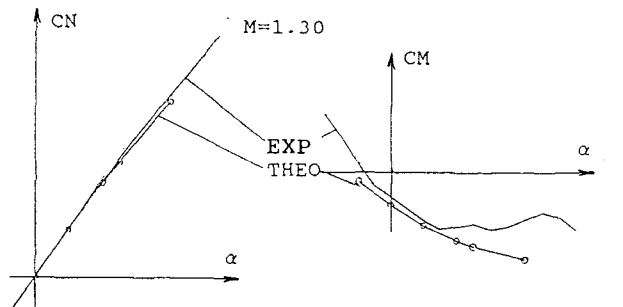


FIG. 30

COMPARISON THEORETICAL TO EXPERIMENTAL RESULTS

Regarding to pressure distributions, the according is good enough for all the subsonic Mach numbers examined at incidences featuring attached flow (fig.31).

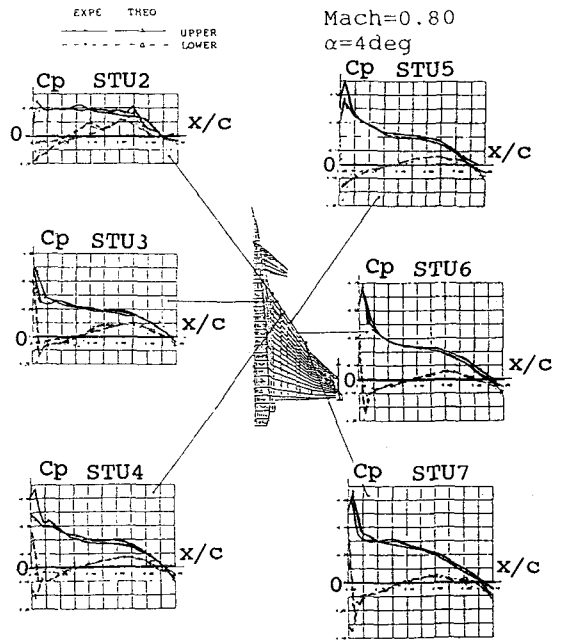


FIG. 31

COMPARISON THEORETICAL TO EXPERIMENTAL RESULTS

As expected, there is no according between experimental data and theoretical predictions, as soon as experimental pressure distributions show vortex onset. In this time, AIT Aerodynamic Design Office is evaluating a higher-order panel code, HISSS, that gives a more accurate prediction of minimum pressure coefficient near l.e. (the "key" parameter of the criterion) to the aim of verifying and implementing in a rational way the complete procedure in the aerodynamic design process.

7. CONCLUSIONS

The detailed analysis of the flow characteristics of a delta canard configuration presented in this paper has been articulated on the comparison of flight data (E.A.P. demonstrator aircraft) and wind tunnel results (E.A.P. Model 9). The study of pressure distribution has been carried out in order to put on evidence the following points.

Emphasis has been given to the transition from attached flow to vortical flow highlighting the effects of this phenomenon on longitudinal coefficients, i.e. on the aircraft aerodynamic characteristics. Particular importance has been devoted to the effects of foreplane on the wing flow field.

Reynolds number effects on pressure and longitudinal coefficients have been analyzed.

The background the prediction criterion is based upon suggests the possibility to utilize "relatively simple and cheap" potential codes to predict transition from attached to vortical flow.

REFERENCES

SALVATORE, A. - FERRETTI, A.
"Applicabilità delle metodologie classiche di determinazione del buffet a configurazioni alari tipo delta - canard"
AIT GAD, Torino, Italy, April 1990

ERICKSON, G.E.
"Vortex flow correlation"
I.C.A.S. paper n°82-6.6.1., August 1982

SZODRUCH, J.
"Delta wing configuration"
M.B.B. Civil Transport Division

STANBROOK, A. - SQUIRE, L.C.
"Possible type of flow at swept leading edges"
Aeronautical Quarterly, vol. 15, 1964

SESHADRI, S.N. - NARAYAN, K.Y.
"Shock induced separated flows on the lee surface of delta wing"
National Aeronautical Laboratory,
Bangalore, India

LOCK, R.C.
"An equivalence law relating three and two dimensional pressure distribution"
ARC R & M 3346, 1962

AA. VV.
"Critical pressure coefficient and component of local Mach number to the surface isobar for a swept wing"
E.S.D.U. 75027, R.A.S., October 1975

KULKAN, R.M. - SIGALLA, A.
"Real flow limitation in supersonic airplane design"
J.AIRCRAFT, vol. 16, n° 10, October 1979

ER EL, J. - YITZHAK, Z.
"Experimental examination of the leading edge suction analogy"
J.AIRCRAFT, vol. 25, n° 3, March 1988

MILLER, D.S. - WOOD, R.M.
"Leeside flows over delta wings at supersonic speeds"
J.AIRCRAFT, vol. 21, n° 9

VERHAAGEN, N.G.
"An experimental investigation of the vortex flow over delta and double delta wings at low speed"
Rep. LR 372, Dept. of Aerospace Engineering, Delft University of Technology

LAMAR, E.J. - CAMPBELL, J.F.
"Recent studies at NASA-Langley of vortical flows interacting with neighboring surfaces"
AGARD

MAUTESE, S.
"Model M 9 - T.W.T. ARA testing comparison of the pressure integration data with the sting balance results"
AIT GAD Torino, Italy, January 1987

MARSDEN, P. - KING, J.N. - CONNOLLY, M.
"Details of tests in the ARA 2.74m * 2.44m transonic wind tunnel on the 1/13 scale E.A.P. Model 9"
Model Test Note Q70/1, ARA, November 1986

JORDAN, R.
"A selection of tabulated results from the experimental data bank of the M 165 canard/wing research model tested in the ARA 9 * 8 ft wind tunnel - Supplied for I.E.P.G. - TA 15"
ARA, Data Note M 165 D.1, D.2, March 1989.